

Three-body interactions with cold polar molecules

H. P. Büchler, A. Micheli, and P. Zoller

*Institute for Theoretical Physics, University of Innsbruck, 6020 Innsbruck, Austria and
Institute for Quantum Optics and Quantum Information, 6020 Innsbruck, Austria*

(Dated: November 4, 2018)

We show that polar molecules driven by microwave fields give naturally rise to strong three-body interactions, while the two-particle interaction can be independently controlled and even switched off. The derivation of these effective interaction potentials is based on a microscopic understanding of the underlying molecular physics, and follows from a well controlled and systematic expansion into many-body interaction terms. For molecules trapped in an optical lattice, we show that these interaction potentials give rise to Hubbard models with strong nearest-neighbor two-body and three-body interaction. As an illustration, we study the one-dimensional Bose-Hubbard model with dominant three-body interaction and derive its phase diagram.

Fundamental interactions between particles, such as the Coulomb law, involves pairs of particles, and our understanding of the plethora of phenomena in condensed matter physics rests on models involving effective two-body interactions. On the other hand, exotic quantum phases, such as topological phases or spin liquids, are often identified as ground states of Hamiltonians with three or more body terms. While the study of these phases and properties of their excitations is presently one of the most exciting developments in theoretical condensed matter physics, it is difficult to identify real physical systems exhibiting such properties - a noticeable exception being the Fractional Quantum Hall effect. Here we show that polar molecules in optical lattices driven by microwave fields give naturally rise to Hubbard models with strong nearest-neighbor three-body interactions, while the two-body terms can be tuned (even switched off) with external fields.

The many-body Hamiltonians underlying condensed matter physics are derived within an effective low energy theory, obtained by integrating out the high energy excitations. In general, this gives rise to interaction terms

$$V_{\text{eff}}(\{\mathbf{r}_i\}) = \sum_{i<j} V(\mathbf{r}_i - \mathbf{r}_j) + \sum_{i<j<k} W(\mathbf{r}_i, \mathbf{r}_j, \mathbf{r}_k) + \dots \quad (1)$$

where $V(\mathbf{r})$ describes the two-particle interaction depending only on the separation between the particles. The second term $W(\mathbf{r}_i, \mathbf{r}_j, \mathbf{r}_k)$ is the three-body interaction, which depends on the distance and orientation of three particles, and vanishes if one particle is far apart from the other two. The ellipsis denotes possible higher many-body terms. While for Helium atoms in the context of superfluidity the two-particle interaction dominates and determines the ground state properties with the three-body interactions providing small corrections,¹ model Hamiltonians with strong three-body interactions have attracted a lot of interest in the search for microscopic Hamiltonians exhibiting exotic ground state properties. Well known examples are the fractional quantum Hall states described by the Pfaffian wave functions which appear as ground states of a Hamiltonian with three-body interaction.^{2,3,4} These topological

phases admit anyonic excitations with non-abelian braiding statistic. Of special interest are also spin systems and bosonic Hamiltonians with complex many-body interactions, such as ring exchange model, which are expected to give rise to exotic phases.^{5,6,7,8} Three-body interactions are also an essential ingredient for systems with a low energy degeneracy characterized by string nets,^{9,10} which play an important role in models for non-abelian topological phases. The main challenge is then to identify experimental accessible systems, where the two-particle interaction $V(\mathbf{r})$ can be controlled, independent of the three-body interaction $W(\mathbf{r}_i, \mathbf{r}_j, \mathbf{r}_k)$.

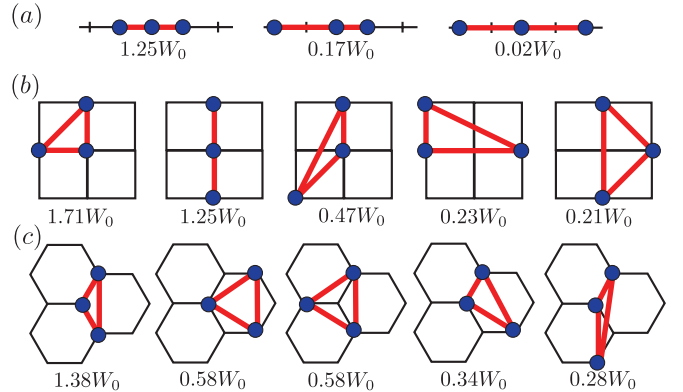


FIG. 1: Strengths of the dominant three-body interactions W_{ijk} appearing in the Hubbard model for different lattice geometries: (a) one-dimensional setup (b) two-dimensional square lattice (c) two-dimensional honeycomb lattice. The characteristic energy scale $W_0 = \gamma_2 DR_0^6/a^6$ is discussed following Eq. (14).

In the present work we analyze the effective interaction potential in a many-body system of polar molecules. Recently, systems of polar molecules in the rovibrational ground state have attracted a lot of interest recently due to their rich internal structure and the presence of large permanent dipole moments, which give rise to dipole-dipole interactions and offer the possibility to tune the interaction with static electric fields and microwave fields.^{11,12,13,14,15,16} The techniques for trapping

and cooling of polar molecules with the goal to create quantum degenerate ground state molecules are currently developed in several laboratories.^{17,18,19,20,21,22,23} We show below that for an appropriate choice of static electric and microwave fields the effective interaction reduces to the form as in Eq. (1) with tunable two-body and the three-body interactions.

In particular, for polar molecules moving in an optical lattice we obtain the Hubbard model

$$H = -J \sum_{\langle ij \rangle} b_i^\dagger b_j + \sum_{i \neq j} \frac{U_{ij}}{2} n_i n_j + \sum_{i \neq j \neq k} \frac{W_{ijk}}{6} n_i n_j n_k. \quad (2)$$

Here b_i (b_i^\dagger) are destruction (creation) operators for a molecule on lattice site i , satisfying canonical commutation (anti-commutation) relations for bosonic (fermionic) molecules, and a hard-core on-site repulsion is implied for bosons. The first term in Eq. (2) is a hopping term (kinetic energy), while the last two terms describe two-body and three-body interaction terms ($n_i = b_i^\dagger b_i$). The different strengths of the three-body interaction terms are illustrated in Fig. 1. We emphasize that our derivation of the Hubbard model Eq. (2), resulting in strong and tunable two and three-body interactions, will be based directly on the effective many-particle potential Eq. (1). This is in contrast to the common approach to derive effective many-body terms from Hubbard models involving two-body interactions, which are obtained in a $J \ll U$ perturbation theory, and are thus necessarily small.²⁴ The main part of the present work is concerned with the microscopic derivation of the Hamiltonian in Eq. (2), and the tunability of the parameters by external fields. As an illustration, we analyze the simplest possible case of a one-dimensional Bose-Hubbard model with a dominant three-body interaction, and derive the phase diagram using Bosonization techniques.

I. EFFECTIVE INTERACTION POTENTIAL

The internal structure of polar molecules with a closed shell electronic structure $^1\Sigma$ is given by the rotational degree of freedom, and its low energy excitations are well described by the rigid rotor Hamiltonian

$$H_{\text{rot}}^{(i)} = B \mathbf{J}_i^2 \quad (3)$$

with B the rotational constant, and \mathbf{J}_i the dimensionless angular momentum operator. Here, we are mainly interested in the ground state $|0, 0\rangle_i$, and the first excited state manifold $|1, m_z\rangle_i$ ($|j, m_z\rangle_i$ denote the eigenstates of the rotor). The rotational levels couple to external electric fields via $H_{\text{ext}}^{(i)} = -\mathbf{d}_i \mathbf{E}(t)$ with \mathbf{d}_i the dipole operator. Under a static electric field $\mathbf{E} = E \mathbf{e}_z$ along the z -axis the degeneracy of the excited state manifold with $j = 1$ is lifted, see Fig. 2. In the following we denote the new dressed states by $|0\rangle_i \rightarrow |g\rangle_i$ for the ground state, $|1, 0\rangle_i \rightarrow |e\rangle_i$ for the state with $m_z = 0$, and

$|1, \pm 1\rangle_i \rightarrow |e_\pm\rangle_i$ for the remaining two degenerate states, and the corresponding energies E_g , E_e , and $E_{e,\pm}$.

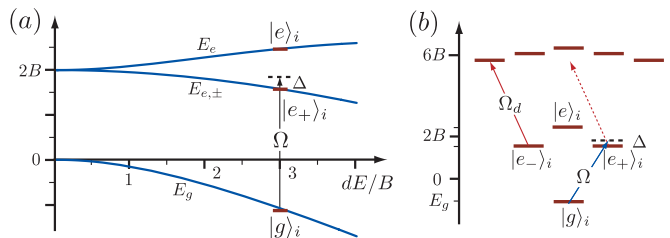


FIG. 2: (a) Internal excitation energies for a single polar molecule in a static electric field $\mathbf{E} = E \mathbf{e}_z$. (b) Level structure for $Ed/B = 3$: the circular polarized microwave field couples the ground state $|g\rangle_i$ with the excited state $|e_+\rangle_i$ with Rabi frequency Ω/\hbar and detuning Δ . Applying a second microwave field with opposite polarization (red arrow) allows us to lift the degeneracy in the first excited manifold ($j = 1$) by resonantly couple the state $|e_-\rangle_i$ to the manifold with $j = 2$.

We focus on a setup with a circular polarized microwave field along the z -axis, which couples the states $|g\rangle_i$ and $|e_+\rangle_i$ with detuning Δ and Rabi frequency Ω/\hbar . We assume that the degeneracy of the states $|e_-\rangle_i$ and $|e_+\rangle_i$ is lifted, e.g., by an additional microwave field coupling the state $|e_-\rangle_i$ near-resonantly to the next state manifold inducing an AC shift, see Fig. 2; the degenerate situation is presented in Appendix A. The internal structure of a single polar molecule is then described as a spin-1/2 particle via the identification of the state $|g\rangle_i$ ($|e_+\rangle_i$) as eigenstates of the spin operator S_i^z with positive (negative) eigenvalue. In the rotating frame and applying the rotating wave approximation, the Hamiltonian describing the internal dynamics of the polar molecule reduces to

$$H_0^{(i)} = \frac{1}{2} \begin{pmatrix} \Delta & \Omega \\ \Omega & -\Delta \end{pmatrix} = \mathbf{h} \mathbf{S}_i \quad (4)$$

with the effective magnetic field $\mathbf{h} = (\Omega, 0, \Delta)$ and the spin operator $\mathbf{S}_i = (S_i^x, S_i^y, S_i^z)$. The eigenstates of this Hamiltonian are denoted as $|+\rangle_i = \alpha|g\rangle_i + \beta|e_+\rangle_i$ and $|-\rangle_i = -\beta|g\rangle_i + \alpha|e_+\rangle_i$ with energies $\pm\sqrt{\Delta^2 + \Omega^2}/2$. In the following, we consider a blue detuned microwave field with $\Delta > 0$, and molecule prepared into the state $|+\rangle_i$. The preparation in this state is obtained by adiabatically turning on the microwave field for molecules initially in their ground state $|g\rangle_i$.

The interaction between the polar molecules is determined by the dipole-dipole interaction

$$V_{\text{d-d}}(\mathbf{r}_{ij}) = \frac{\mathbf{d}_i \mathbf{d}_j}{|\mathbf{r}_{ij}|^3} - \frac{3(\mathbf{r}_{ij} \mathbf{d}_i)(\mathbf{r}_{ij} \mathbf{d}_j)}{|\mathbf{r}_{ij}|^5} \quad (5)$$

with $\mathbf{r}_{ij} = \mathbf{r}_i - \mathbf{r}_j$ the separation between the particles. In the interesting regime with $|\mathbf{r}_{ij}| \gg (D/B)^{1/3}$, the dipole-dipole interaction restricted to the internal states $|e_+\rangle_i$ and $|g\rangle_i$ expressed in the rotating frame, and applying the

rotating wave approximation reduces to $H_d = H_d^{\text{ex}} + H_d^{\text{dc}}$. The first term takes the form ($S_i^{\pm} = S_i^x \pm iS_i^y$)

$$H_d^{\text{ex}} = -\frac{1}{2} \sum_{i \neq j} \frac{D}{2} \nu(\mathbf{r}_{ij}) [S_i^+ S_j^- + S_j^+ S_i^-] \quad (6)$$

with the dipole coupling $D = |\langle g | \mathbf{d}_i | e_+ \rangle|^2$, while the induced dipole moments $d_g = \partial_E E_g$ and $d_e = \partial_E E_{e,+}$ gives rise to a second term

$$H_d^{\text{dc}} = \frac{1}{2} \sum_{i \neq j} D \nu(\mathbf{r}_{ij}) [\eta_g P_i + \eta_e Q_i] [\eta_g P_j + \eta_e Q_j]. \quad (7)$$

Here, $P_i = 1/2 + S_i^z$ and $Q_i = 1/2 - S_i^z$ are the projectors on the ground and excited states, while $\eta_g = d_g/\sqrt{D}$ and $\eta_e = d_e/\sqrt{D}$ are the dipole couplings. The anisotropic behavior of the dipole-dipole interaction is accounted for by $\nu(\mathbf{r}) = (1 - 3 \cos^2 \theta)/r^3$ with θ the angle between \mathbf{r} and the z -axis.

Next, we are interested in the effective interaction between the polar molecules with each molecule prepared in the state $|+\rangle_i$. Within the Born-Oppenheimer approximation, we determine the eigenenergies of the internal Hamiltonian $\sum_i H_0^{(i)} + H_d$ for fixed particle positions $\{\mathbf{r}_i\}$, and obtain the energy shift of the state adiabatically connected to the state $|G\rangle = \Pi_i |+\rangle_i$ of the non-interacting system. This energy shift is driven by the dipole-dipole interaction H_d and strongly depends on the positions of the particles $\{\mathbf{r}_i\}$ and therefore describes the effective interaction $V_{\text{eff}}(\{\mathbf{r}_i\})$. In the following, we derive this energy shift using perturbation theory in the dipole-dipole interaction H_d , and derive the effective interaction potentials. The small parameter controlling the perturbative expansion is $D/(a^3 |\mathbf{h}|) = (R_0/a)^3$ with a the characteristic length scale of the interparticle separation, $|\mathbf{h}| = \sqrt{\Delta^2 + \Omega^2}$ the strength of the effective magnetic field, and the length scale $R_0 = (D/\sqrt{\Delta^2 + \Omega^2})^{1/3}$. In first order perturbation theory, we obtain the energy correction

$$E^{(1)}(\{\mathbf{r}_i\}) = \frac{1}{2} \left[(\alpha^2 \eta_g + \beta^2 \eta_e)^2 - \alpha^2 \beta^2 \right] \sum_{i \neq j} D \nu(\mathbf{r}_{ij}), \quad (8)$$

which describes a dipole-dipole interaction between the particles. In addition, the energy shift in second order perturbation theory reduces to

$$E^{(2)}(\{\mathbf{r}_i\}) = \sum_{k \neq i, k \neq j} \frac{|M|^2}{\sqrt{\Delta^2 + \Omega^2}} D^2 \nu(\mathbf{r}_{ik}) \nu(\mathbf{r}_{jk}) + \sum_{i < j} \frac{|N|^2}{2\sqrt{\Delta^2 + \Omega^2}} [D \nu(\mathbf{r}_{ij})]^2. \quad (9)$$

and gives rise to a correction to the two-particle interaction potential and an additional three-body interaction. The matrix elements M and N take the form

$$M = \alpha \beta [(\alpha^2 \eta_g + \beta^2 \eta_e)(\eta_e - \eta_g) + (\beta^2 - \alpha^2)/2], \\ N = \alpha^2 \beta^2 [(\eta_e - \eta_g)^2 + 1].$$

Therefore, the effective interaction potential V_{eff} up to second order in $(R_0/a)^3$ reduces to the form in Eq. (1) with the two-particle interaction potential

$$V(\mathbf{r}) = \lambda_1 D \nu(\mathbf{r}) + \lambda_2 D R_0^3 [\nu(\mathbf{r})]^2, \quad (10)$$

and the three-body interaction

$$W(\mathbf{r}_1, \mathbf{r}_2, \mathbf{r}_3) = \gamma_2 R_0^3 D [\nu(\mathbf{r}_{12}) \nu(\mathbf{r}_{13}) + \nu(\mathbf{r}_{12}) \nu(\mathbf{r}_{23}) + \nu(\mathbf{r}_{13}) \nu(\mathbf{r}_{23})]. \quad (11)$$

The dimensionless coupling parameters are $\lambda_1 = (\alpha^2 \eta_g + \beta^2 \eta_e)^2 - \alpha^2 \beta^2$, $\lambda_2 = 2|M|^2 + |N|^2/2$, and $\gamma_2 = 2|M|^2$. These parameters can be tuned via the strength of the electric field Ed/B and the ratio between the Rabi frequency and the detuning, Ω/Δ , see Fig. 3. Of special interest are the values of the external fields, where $\lambda_1 = 0$, i.e., the leading two-particle interaction vanishes. Then, the interaction is dominated by the second order contribution with λ_2 and γ_2 , which includes the three-body interaction, see Fig. 3d, while small deviation away from the line $\lambda_1 = 0$ allows us to change the character of the two-particle interaction. Note, that a n -body interaction term ($n \geq 4$) appears in $(n-1)$ -th order perturbation theory in the small parameter $(R_0/a)^3$. Therefore, the contribution of these terms is suppressed and can be safely ignored in our context.

The above analysis for $|G\rangle = \Pi_i |+\rangle$ ($\Delta > 0$) provides a positive energy shift in second order $E^{(2)}(\{\mathbf{r}_i\})$, as $|G\rangle$ corresponds to the highest energy state, and provides a repulsive interaction with $\lambda_2 \geq 0$ and $\gamma_2 \geq 0$. In turn, in an analogous analysis for the lowest energy state $\Pi_i |-\rangle$, $E^{(2)}$ is negative, which yields a change of sign of the coupling parameters λ_2 and γ_2 .

The validity of the effective interaction $V_{\text{eff}}(\{\mathbf{r}_i\})$ is restricted to interparticle distances $|\mathbf{r}_i - \mathbf{r}_j| > R_0$. Here, we prevent particles to approach each other on shorter distances $|\mathbf{r}_i - \mathbf{r}_j| < R_0$ by focusing on setups where the combination of interparticle potential for $|\mathbf{r}_i - \mathbf{r}_j| > R_0$ and the transverse trapping potential produces a strong repulsive barrier. For sufficiently strong barrier height, thermal activation across the barrier and quantum mechanical tunneling through the barrier are then suppressed, and the particles are confined in parameter space to the region $|\mathbf{r}_i - \mathbf{r}_j| > R_0$. A setup providing such a barrier is obtained by confining the particles into two-dimensions by a strong transverse trapping potential along the z -axis with transverse trapping frequency $\omega_{\perp} = \hbar/m a_{\perp}^2$ as provided for example by an optical lattice. The condition for an efficient barrier in this two-dimensional setup has been recently worked out for polarized molecules with leading dipole-dipole interaction.^{25,26} However, the analysis can be generalized to the present situation with the interaction potential $V_{\text{eff}}(\{\mathbf{r}_i\})$, if the two-particle potential $V(\mathbf{r})$ is sufficient repulsive, i.e., $\lambda_1 \gtrsim -\lambda_2 (R_0/a)^3$. For $\hbar \omega_{\perp} > D/R_0^3$, an estimate of the rate for two-particles to penetrate the barrier up to a distance $|\mathbf{r}_i - \mathbf{r}_j| < R_0$ is provided by $\Gamma \sim (\hbar/m a^2) \exp(-2S_E/\hbar)$ with the semiclassical

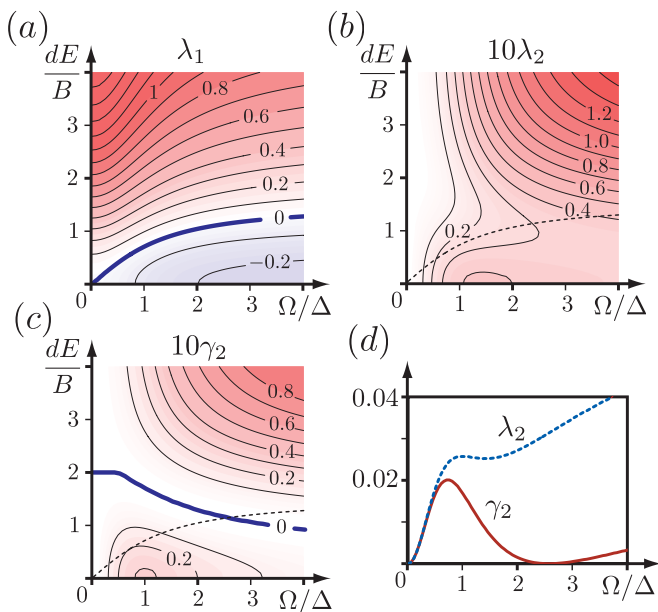


FIG. 3: (a)-(c) Strength of the interaction parameters λ_1 , λ_2 , and γ_2 as a function of the external fields Ed/B and Ω/Δ . The leading dipole-dipole interaction vanishes for $\lambda_1 = 0$ (dashed line in (b) and (c)), and the second order contributions dominate the interaction. (d) Strength of λ_2 (dashed line) and γ_2 (solid line) along the line in parameter space with $\lambda_1 = 0$.

sical action $S_E/\hbar \sim \sqrt{Dm/R_0\hbar^2}$. This exponential suppression confines particle in parameter space to the region $|\mathbf{r}_i - \mathbf{r}_j| > R_0$ for realistic parameters with polar molecules, see below.

The low-energy many-body theory now follows by combining the kinetic energy of the polar molecules with the effective interaction V_{eff} within the Born-Oppenheimer approximation and the external trapping potentials V_T

$$H = \sum_i \frac{\mathbf{p}_i^2}{2m} + V_{\text{eff}}(\{\mathbf{r}_i\}) + \sum_i V_T(\mathbf{r}_i). \quad (12)$$

Note, that the Hamiltonian is independent of the statistics of the particles and therefore, valid for bosonic and fermionic polar molecules. In the strongly interacting regime, where the interaction energy dominates over the kinetic energy, it is expected that the ground state of the many-body system is determined by crystalline phases.²⁵

II. HUBBARD MODEL

Applying an optical lattice provides a periodic structure for the polar molecules described by the Hamiltonian Eq. (12) and allows us to derive Hubbard models with unconventional and strong nearest-neighbor interactions. We focus on the above setup, where the stability of the system is obtained by a strong transverse

trapping potential. We describe the lattice structure with lattice spacing a by a set of vectors $\{\mathbf{R}_i\}$ accounting for the minima of the optical lattice; depending on the optical lattice, we can generate one-dimensional and two-dimensional systems. The mapping to the Hubbard model follows the standard procedure:²⁷ (i) Solving the single particle problem in the presence of the optical lattice provides the Wannier functions $w(\mathbf{r})$ for the lowest Bloch band and determines the hopping energy J . The Wannier functions describe localized wave functions with characteristic size a_0 . (ii) We express the field operator ψ in terms of the Wannier functions in the lowest band $\psi^\dagger(\mathbf{r}) = \sum_i w(\mathbf{r} - \mathbf{R}_i)b_i^\dagger$ with b_i^\dagger (b_i) the creation (annihilation) operator at the lattice site \mathbf{R}_i . In order to simplify the discussion, we consider bosonic particles satisfying bosonic commutation relations. Expressing the Hamiltonian Eq. (12) in second quantization and inserting the bosonic field operator ψ , maps the system to the Bose-Hubbard model. However, the on-site interaction, which derives for cold atomic gases from the pseudopotential, requires a special discussion in the present situation. In the experimentally interesting regime, we have the following separation of the length scales: $a_0 \leq R_0 < a$. With the above discussion, that the parameter space of the system is confined to interparticle distances larger than R_0 , this implies that if a particle is at site \mathbf{R}_i , the hopping rate for a second particle to tunnel to this site is strongly suppressed. As the initial system has no doubly occupied sites, a convenient way to express this conditional hopping is to describe the bosons as hard-core bosons. Consequently, no on-site interaction term is present, and we obtain the Bose-Hubbard model in Eq. (2). The interaction parameters U_{ij} and V_{ijk} derive from the effective interaction $V(\{\mathbf{r}_i\})$, and in the limit of well-localized Wannier functions ($a_0/a \ll 1$) reduce to $U_{ij} = V(\mathbf{R}_i - \mathbf{R}_j)$ and $W_{ijk} = W(\mathbf{R}_i, \mathbf{R}_j, \mathbf{R}_k)$. The decay of these interactions with interparticle separation takes the form

$$U_{ij} = U_0 \frac{a^3}{|\mathbf{R}_i - \mathbf{R}_j|^3} + U_1 \frac{a^6}{|\mathbf{R}_i - \mathbf{R}_j|^6}, \quad (13)$$

$$W_{ijk} = W_0 \left[\frac{a^6}{|\mathbf{R}_i - \mathbf{R}_j|^3 |\mathbf{R}_i - \mathbf{R}_k|^3} + \text{perm} \right]. \quad (14)$$

Here, $U_0 = \lambda_1 D/a^3$, $U_1 = \lambda_2 D R_0^3/a^6$, and $W_0 = \gamma_2 D R_0^3/a^6$ denote characteristic energy scales. The dominant contributions and strengths of the three-body terms in different lattice geometries are shown in Fig. 1.

In the following, we estimate these energy scales for LiCs with a permanent dipole moment $d = 6.3$ Debye. Assuming an optical lattice with lattice spacing $a \approx 500$ nm, the characteristic dimensionless parameter determining the ratio between the interaction energy ($E_{\text{int}} = D/a^3$) and the characteristic kinetic energy within the lattice ($E_{\text{kin}} = \hbar^2/ma^2$ proportional to the recoil energy) becomes $r_d = Dm/\hbar^2 a \approx 55$. The leading dipole-dipole interaction can give rise to very strong nearest-neighbor interactions with $U_0 \sim 55 E_{\text{kin}}$. On the other hand, tuning the parameters via the external fields to $\lambda_1 = 0$ the

	u	β
$n = 1/3$	Wa/π	$\sqrt{36\pi}$
$n = 1/2$	$Wa/2$	$\sqrt{16\pi}$
$n = 2/3$	Wa/π	$\sqrt{36\pi}$

TABLE I: Parameters of the sine-Gordon term

characteristic energy scale for the three-body interaction becomes $W_0 \approx (R_0/a)^3 E_{\text{kin}}$. Then, controlling the hopping energy J via the strength of the optical lattice allows us to enter the regime with dominant the three-body interactions.

III. THREE-BODY INTERACTIONS IN 1D

As an illustration, we study the one-dimensional system with leading three-body interaction. Tuning the external fields to a point with $U_1 = -U_0$, the Hamiltonian takes the form

$$H = -J \sum_i [b_i^\dagger b_{i+1} + b_{i+1}^\dagger b_i] + W \sum_i n_{i-1} n_i n_{i+1}, \quad (15)$$

where we have kept only the nearest-neighbor terms. The additional interaction terms play a minor role in the following analysis. Using a Jordan-Wigner transformation allows us to map the hard-core bosons onto an interacting Fermi system, which can be studied using Bosonization techniques;^{28,29} the details of the calculation are presented in Appendix B. As a final result, we obtain that the low energy Hamiltonian is described by the sine-Gordon model for the particle densities $n = 1/3$, $n = 1/2$, and $n = 2/3$,

$$H = \frac{\hbar v}{2} \int dx \left[K \Pi^2 + \frac{1}{K} (\partial_x \Phi)^2 \right] + u \int dx \frac{1}{\pi^2 a^2} \cos(\beta \Phi). \quad (16)$$

The parameters u and β for the sine term are given in Table I. The renormalized Fermi velocity is $v = 2Ja \sin(\pi n)/\hbar K$, while the dimensionless Luttinger parameter takes the form $K = 1/\sqrt{1+\kappa}$ with

$$\kappa = \frac{W}{2J} \frac{2n}{\pi} \frac{3 - 2 \cos(2\pi n) - \cos(4\pi n)}{\sin(\pi n)} \quad (17)$$

The Hamiltonian Eq. (16) allows now for the derivation of the expected phases diagram.

For weak interactions $W/2J < 1$, the three-body interaction shifts the hard-core bosons away from the Tonks gas limit ($K = 1$) into the correlated regime with $K < 1$. This regime is characterized by algebraic correlation functions, e.g., the off-diagonal correlation between the bosons decays as $\langle b_i b_j^\dagger \rangle \sim |i-j|^{-1/2K}$, and the density-density correlation $\langle (n_i - n)(n_j - n) \rangle \sim \cos[2\pi n(i-j)]/|i-j|^{2K}$.³⁰ At three values of the density $n = 2/3$, $n = 1/2$, and $n = 1/3$, the sine-Gordon term drives an instability towards a gapped phase, see

Fig. 4. The critical value K for this instability is given by $K = 8\pi/\beta^2$. In the following, we use this criterion to identify the instabilities towards three solid phases for $W/2J \sim 1$; the exact determination of the critical interaction strength requires an analysis beyond the scope of this paper. These solid phases are characterized by a broken translational symmetry, where the following observables allow us to distinguish the different ground states

$$\langle n_j \rangle \sim \cos \left[2\pi j n + \sqrt{4\pi} \Phi_l \right], \quad (18)$$

$$\langle b_j b_{j+1}^\dagger + b_j^\dagger b_{j+1} \rangle \sim \cos \left[(2\pi j + \pi)n + \sqrt{4\pi} \Phi_l \right] \quad (19)$$

with Φ_l characterizing the different ground states. The first observable describes a density wave with wave vector $k = 2\pi n/a$ present in conventional solids, while the second observable accounts for a bond order with wave vector $k = 2\pi n/a$, see Fig. 4b for an illustration of the different order appearing in the ground state.

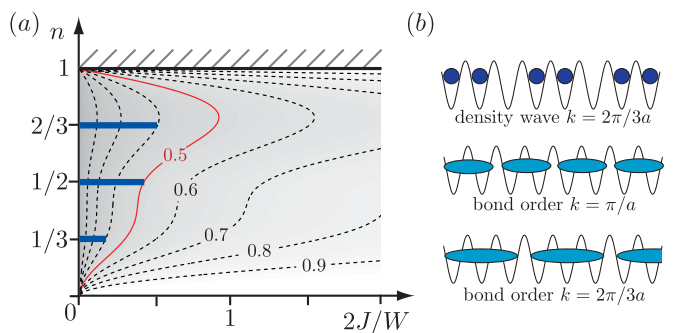


FIG. 4: (a) Sketch of the W/J - n phase diagram: The dashed contours correspond to constant values of K . The first instability at $n = 1/2$ appears for $K = 1/2$ (thin solid line), while the instabilities at $n = 1/3$ and $n = 2/3$ appear at lower values of K . Note that the interaction strength approaches $W/2J \approx 1$ at the position of the instabilities, and we expect the exact position of the instability to be strongly renormalized. (b) Illustration of the three different solid order characterizing the gapped phases: density order with wave vector $k = 2\pi/3a$, bond order with $k = \pi/a$, and bond order with wave vector $k = 2\pi/3a$.

At half filling $n = 1/2$, the instability towards a gapped phase appears for $K = 1/2$. Within the gapped phase, the sine-Gordon term in Eq. (16) determines the long-distance behavior, and the phase field Φ is predominantly pinned within a minimum of the $\cos(\sqrt{16\pi}\Phi)$ term. The minima take the form $\Phi_l = \pi(2l+1)/\sqrt{16\pi}$, and characterize the different ground states in the gapped phase. These ground state can be distinguished by the bond observable in Eq. (19). Therefore, we obtain a two-fold degenerate phase with a broken translational symmetry: the bond correlation function exhibits a long range order at the wave vector $k = \pi/a$, while the density $\langle n_j \rangle$ remains uniform in this phase. The corresponding phase in spin systems is denoted as a spin-Peierls phase.²⁹

In turn, for the densities $n = 1/3$ and $n = 2/3$ the instability appears at lower values of K . The ground states of the gapped phase are then characterized by the minima of $\cos(\sqrt{36\pi}\Phi)$, which are given by $\Phi_l = \pi(2l+1)/\sqrt{36\pi}$. The different ground states can be distinguished by the density and bond observable providing a three-fold degenerate phase with a density wave and a bond order at the wave vector $k = 2\pi/3$. The appearance of a density wave with $k = 2\pi/3$ is a special property of the three-body interaction. It can be well understood for $n = 2/3$ in the limit $W/2J \gg 1$: then the ground state takes the form $\prod_i b_{3i}^\dagger b_{3i+1}^\dagger |0\rangle$ and describes a perfect density wave.

Within the above Bosonization approach, the additional interaction terms beyond nearest-neighbor three-body interaction only provide a small renormalization of the coupling parameters in Eq. (16), and therefore play a minor role in the qualitative discussion of the instabilities. However, in the limit $W/2J \gg 1$ they become important and can give rise to additional solid phases.

IV. CONCLUSIONS AND OUTLOOK

A many-body system of cold polar molecules, whose rotational states are dressed by an external static electric field and microwave field, can be described by an effective Hamiltonian, where three-body interactions play the dominant role. The derivation of this effective Hamiltonian involving interaction potentials as a series of two-body, three-body etc. interactions is based on a microscopic understanding of the underlying molecular physics, and is systematic in the sense that the series expansion is well controlled. A unique feature of the system is that, as a function of the external fields, the two-body interactions can be tuned from repulsive to attractive, and even switched off, while the three-body terms remain repulsive and strong. For molecules trapped in an optical lattice this leads to Hubbard models with tunable nearest neighbor two-body interactions and repulsive three-body terms. Models of this type have appeared in the recent discussion of exotic quantum phases, in particular in the context of topological quantum phases and quantum computing, and we see molecular quantum gases as a realistic experimental route, which provides the basic building blocks and techniques towards the study of these phenomena.

APPENDIX A: DEGENERATE STATES

For a setup with $|e_+\rangle_i$ and $|e_-\rangle_i$ degenerate, it is necessary to keep the three states $|+\rangle_i$, $|-\rangle_i$, and $|e_-\rangle_i$ for the perturbative calculation of the Born-Oppenheimer potentials. The leading contribution $E_1(\{\mathbf{r}_i\})$ is not modified, while the following term in the dipole-dipole interaction provides a non-vanishing contribution in second

order perturbation theory,

$$\Delta H_d^{\text{ex}} = \frac{1}{2} \sum_{i \neq j} D [\mu(\mathbf{r}_{ij})]^* T_i^+ S_j^- + \mu(\mathbf{r}_{ij}) T_i^- S_j^+ \quad (\text{A1})$$

with the operators $T_i^+ = |e_-\rangle\langle g|$ and $T_i^- = |g\rangle\langle e_-|$ coupling the ground state with the excited state and the potential $\mu(\mathbf{r}) = -3(x - iy)^2/2r^5$. We therefore obtain a correction to the two-body interaction potential

$$\Delta V(\mathbf{r}) = \lambda_3 D R_0^3 |\mu(\mathbf{r})|^2, \quad (\text{A2})$$

and the three-body interaction

$$W(\mathbf{r}_1, \mathbf{r}_2, \mathbf{r}_3) = \gamma_3 \frac{D R_0^3}{2} \sum_{i \neq j \neq k}^3 [\mu(\mathbf{r}_{ik})]^* \mu(\mathbf{r}_{jk}). \quad (\text{A3})$$

The dimensionless parameters λ_3 and γ_3 take the form

$$\lambda_3 = 2\beta^4 \alpha^2 \frac{\sqrt{\Omega^2 + \Delta^2}}{\Delta + 3\sqrt{\Omega^2 + \Delta^2}} + 4\alpha^4 \beta^2 \frac{\sqrt{\Omega^2 + \Delta^2}}{\Delta + \sqrt{\Delta^2 + \Omega^2}},$$

$$\gamma_3 = 4\alpha^4 \beta^2 \frac{\sqrt{\Omega^2 + \Delta^2}}{\Delta + \sqrt{\Delta^2 + \Omega^2}},$$

and depend on the external fields Ed/B and Ω/Δ .

APPENDIX B: BOSONIZATION

Using the equivalence between hard-core bosons and a spin-1/2 systems, allows us to map the Hamiltonian in Eq. (15) to a fermionic model with Fermi operators c_i (c_i^\dagger) via a Jordan-Wigner transformation. Following the standard Bosonization procedure, we express the fermionic operators via slowly varying left and right moving fields^{28,29}

$$c_i \sim \sqrt{a} [e^{-ik_F x_i} R(x) + e^{ik_F x_i} L(x)] \quad (\text{B1})$$

with $k_F = \pi n/a$ the Fermi momentum and n the averaged particle density. Here, x_i describes the position of the lattice site i , while a denotes the lattice spacing. The fields $R(x)$ and $L(x)$ are slowly varying and smooth on distances a in the continuous variable $x \sim x_i$ with

$$R(x) = \frac{1}{\sqrt{2\pi a}} \exp(i\sqrt{4\pi}\phi) \quad (\text{B2})$$

$$L(x) = \frac{1}{\sqrt{2\pi a}} \exp(-i\sqrt{4\pi}\bar{\phi}). \quad (\text{B3})$$

Then, the Hamiltonian for non-interacting fermions maps to the Luttinger liquid Hamiltonian

$$H_0 = \frac{v_F \hbar}{2} \int dx [\Pi^2 + (\partial_x \Phi)^2] \quad (\text{B4})$$

with the bosonic field $\Phi = \phi + \bar{\phi}$ and Π the momentum conjugate satisfying the canonical commutation relation

$[\Phi(x), \Pi(x')] = i\delta(x - x')$. Here, $v_F = 2J \sin(\pi n)/\hbar$ denotes the Fermi velocity of the non-interacting Fermi system. In order to study the influence of the three-body interaction, we split the density operator n_i into its mean value and the fluctuations, i.e., $n_i = n + \Delta n_i$. Then, the interaction Hamiltonian reduces to $H_{\text{int}} = H_1 + H_2 + H_3$ with

$$H_2 = Wn \sum_i [2\Delta n_i \Delta n_{i+1} + \Delta n_{i-1} \Delta n_{i+1}], \quad (\text{B5})$$

$$H_3 = W \sum_i \Delta n_{i-1} \Delta n_i \Delta n_{i+1}, \quad (\text{B6})$$

while H_1 denotes a shift in the chemical potential and can be dropped. The density operator expressed in the right and left moving fields takes the form

$$\Delta n_i = a [\partial_x \Phi + e^{2ik_F x_i} M^+(x) + e^{-2ik_F x_i} M^-(x)]$$

with

$$M^+(x) =: R^\dagger(x)L(x) :, \quad M^-(x) =: L^\dagger(x)R(x) :.$$

Expressing the interaction Hamiltonian H_{int} in terms of the bosonic fields Φ , special care has to be taken due to the normal ordering $: \cdot :$ of the operators. Furthermore, we note that some terms exhibit a fast oscillations, which can be ignored in the low energy Hamiltonian. Then, the interaction Hamiltonian H_2 takes the form

$$H_{\text{int}} = Wna \int dx \frac{1}{\pi} [3 - 2 \cos(2\pi n) - \cos(4\pi n)] (\partial_x \Phi)^2.$$

Furthermore, at half filling with $n = 1/2$ an additional term appears due to cancellation of different oscillating terms, which takes the sine-Gordon form

$$H_{sG} = u \int dx \frac{1}{\pi^2 a^2} \cos(\beta \Phi) \quad (\text{B7})$$

with $u = Wna$ and $\beta = \sqrt{16\pi}$. The interaction H_3 only contributes less relevant terms, except at fillings $n = 1/3$ and $n = 2/3$. Then an additional terms appears, which takes the sine-Gordon form in Eq. (B7) with parameters $u = Wa/\pi$ and $\beta = \sqrt{36\pi}$.

ACKNOWLEDGMENTS

This work was supported by the Austrian Science Foundation (FWF), the European Union projects OLAQUI (FP6-013501-OLAQUI), CONQUEST (MRTN-CT-2003-505089), the SCALA network (IST-15714), the Institute for Quantum Information, and in part by the National Science Foundation under Grant No. PHY05-51164.

-
- ¹ R. D. Murphy and J. A. Barker, Phys. Rev. A **3**, 1037 (1971).
- ² R. Moore and N. Read, Nucl. Phys. B **360**, 362 (1991).
- ³ E. Fradkin, C. Nayak, A. Tsvelik, and F. Wilczek, Nucl. Phys. B **516**, 704 (1998).
- ⁴ N. R. Cooper, Phys. Rev. Lett. **92**, 220405 (2004).
- ⁵ R. Moessner and S. L. Sondhi, Phys. Rev. Lett. **86**, 1881 (2001).
- ⁶ L. Balents, M. P. A. Fisher, and S. M. Girvin, Phys. Rev. B **65**, 224412 (2002).
- ⁷ O. I. Motrunich and T. Senthil, Phys. Rev. Lett. **89**, 277004 (2002).
- ⁸ M. Hermele, M. P. A. Fisher, and L. Balents, Phys. Rev. B **69**, 064404 (2004).
- ⁹ M. A. Levin and X. G. Wen, Phys. Rev. B **71**, 045110 (2005).
- ¹⁰ L. Fidkowski, M. Freedman, C. Nayak, K. Walker, and Z. Wang, arXiv:cond-mat/0610583 (2006).
- ¹¹ S. Ronen, D. C. E. Bortolotti, D. Blume, and J. L. Bohn, Phys. Rev. A **74**, 033611 (2006).
- ¹² S. Kotochigova and E. Tiesinga, Phys. Rev. A **73**, 041405(R) (2006).
- ¹³ A. Micheli, G. K. Brennen, and P. Zoller, Nature Physics **2**, 341 (2006).
- ¹⁴ M. A. Baranov, K. Osterloh, and M. Lewenstein, Phys. Rev. Lett. **94**, 070404 (2005).
- ¹⁵ D.-W. Wang, M. D. Lukin, and E. Demler, Phys. Rev. Lett. **97**, 180413 (2006).
- ¹⁶ L. Santos, G. V. Shlyapnikov, and M. Lewenstein, Phys. Rev. Lett. **90**, 250403 (2003).
- ¹⁷ J. Doyle, B. Friedrich, R. V. Krems, and F. Masnou-Seeuws, Eur. Phys. J. D **31**, 149 (2004).
- ¹⁸ J. M. Sage, S. Sainis, T. Bergeman, and D. DeMille, Phys. Rev. Lett. **94**, 203001 (2005).
- ¹⁹ T. Rieger, T. Junglen, S. A. Rangwala, P. W. H. Pinkse, and G. Rempe, Phys. Rev. Lett. **95**, 173002 (2005).
- ²⁰ D. Wang, J. Qi, M. F. Stone, O. Nikolayeva, . W. H. B. Hattaway, S. D. Gensemer, P. L. Gould, E. E. Eyler, and W. C. Stwalley, Phys. Rev. Lett. **93**, 243005 (2005).
- ²¹ S. Y. T. van de Meerakker, P. H. M. Smeets, N. Vanhaecke, R. T. Jongma, and G. Meijer, Phys. Rev. Lett. **94**, 23004 (2005).
- ²² S. D. Kraft, P. Staanum, J. Lange, L. Vogel, R. Wester, and M. Weidemüller, J. Phys. B: At. Mol. Opt. Phys. **39** (2006).
- ²³ B. C. Sawyer, B. L. Lev, E. R. Hudson, B. K. Stuhl, M. Lara, J. L. Bohn, and J. Ye, arXiv:physics/0702146 (2007).
- ²⁴ S. Tewari, V. W. Scarola, T. Senthil, and S. D. Sarma, Phys. Rev. Lett. **97**, 200401 (2006).
- ²⁵ H. P. Büchler, E. Demler, M. Lukin, A. Micheli, N. Prokof'ev, G. Pupillo, and P. Zoller, Phys. Rev. Lett.

- 98**, 060404 (2007).
- ²⁶ A. Micheli, G. Pupillo, H. P. Büchler, and P. Zoller, arXiv:quant-ph/0703031 (2007).
- ²⁷ D. Jaksch, C. Bruder, J. I. Cirac, C. W. Gardiner, and P. Zoller, Phys. Rev. Lett. **81**, 3108 (1998).
- ²⁸ A. O. Gogolin, A. A. Nersesyan, and A. M. Tsvelik, *Bosonization and Strongly Correlated Systems* (Cambridge University Press, 1998).
- ²⁹ S. Sachdev, *Quantum Phase Transitions* (Cambridge University Press, 1999).
- ³⁰ F. D. M. Haldane, Phys. Rev. Lett. **47**, 1840 (1981).